Thermal coupling studies of a high temperature proton exchange membrane fuel cell stack and a metal hydride hydrogen storage system

E. Harikishan Reddy[a, b], S. Jayanti [a]*

aDepartment of Chemical Engineering, IIT Madras, India
bDepartment of Chemical Engineering, IIT Hyderabad, India

Abstract

High temperature polymer electrolyte membrane fuel cells (HT-PEMFC) are promising candidates for simple and efficient stand-alone power generation systems. In spite of their relatively high efficiencies, especially at part load conditions, more than half of the chemical energy is converted into thermal energy during the electrochemical generation of electrical power. For stable and efficient operation, it is necessary to remove this heat efficiently and supply pre-heated reactants so as to minimize temperature variations within the cell. In the present study, we explore the possibility of using cathode air to act as coolant of the cell as well as the supplier of the heat required for hydrogen desorption from a sodium alanate-based hydrogen storage system. To this end, we use computational fluid dynamics to simulate the flow and heat transfer through a section of a 1 kWe HT-PEMFC stack and a thermally coupled hydrogen storage system. The calculations show that, with a cathode air flow rate seven times in excess of the stoichiometric requirement, it is possible to meet the triple requirement of supplying preheated cathode air; maintaining uniform stack temperature; and supplying the heat required for desorption of the required amount of H_2.

1. Introduction

Increase in fossil fuel consumption has been reported to have an adverse effect on the climate changes worldwide. There is a pressing need for the development of automotive applications based on hydrogen-

* Corresponding author. Tel.: +91- 44- 2257 4168; fax: 91-44-2257-4152.
  E-mail address: sjayanti@iitm.ac.in.

driven fuel cells. High temperature proton exchange member fuel cells (HT-PEMFCs) offer several advantages in the transportation sector due to their high temperature operation (100-200°C) compared to low temperature proton exchange membrane fuel cells (LT-PEMFCs) [1]. The HT-PEMFC does not require humidification of the reactants during the operation, and allows use of wide range of fuels. It also produces more than half of the thermal energy as by product at the useful temperature of 150°C or higher.

Nomenclature

F	Faraday constant (C /mol)
i	Current density (A /m^2)
I	Current (A)
io	Exchange current density (A /m^2)
n	Number of electrons in electrochemical reaction
Ncell	Number of cells
Q	Thermal energy produced by reaction (W)
Qirrev	Irreversible heat of reaction (W)
Qrev	Reversible heat of reaction (W)
T	Temperature (K)
V	Voltage (V)
$\Delta H_{g,T}$	Enthalpy of water formation in gas phase (J)
ΔH_l^f	Enthalpy of water formation in liquid phase (J)
ΔH_T^{vap}	Enthalpy of vaporization (J)
ΔG_T	Gibbs free energy (J)
ΔH_T	Enthalpy of water formation (J)
ΔS_T	Entropy of reaction (J /K)
ΔT	Temperature difference (K)

Subscripts

Bch1	Bipolar cathode channel of cell-1
Bch2	Bipolar cathode channel of cell-2
Cat1	Cathode catalyst layer of cell-1
Cat2	Cathode catalyst layer of cell-2
Cell	Single cell
CP	Cooling channel
St	Stack

This thermal energy produced from HT-PEMFCs can be utilized for the other process like on-board fuel reformer, hydrogen storage. All these factors make the overall efficiency of the HT-PEMFCs stack higher compared to LT-PEMFCs stack. PEM fuel cells need continuous supply of hydrogen in order produce electrical power. Possible ways of fuel supply for fuel cells for automobile engines is either stored hydrogen or hydrogen produced from an on-board fuel reformer. Hydrogen storage in form of metal hydrides is one of the best options among storage methods, due to their high volumetric capacity and high safety during storage. Typically, hydrogen is stored in a metal hydrate such as sodium alanate ($NaAlH_4$) with a doped catalyst such as cerium. Sodium alanate ($NaAlH_4$) doped with cerium catalyst has fast hydrogen absorption and desorption kinetics as shown reactions below.

$$3NaAlH_4 \quad \leftrightarrow \quad Na_3AlH_6 + 2Al + 3H_2 \tag{1}$$

$$Na_3AlH_6 \leftrightarrow 3NaH + Al + 1.5\ H_2 \tag{2}$$

$$3NaH \qquad \leftrightarrow \quad 3Na + 1.5H_2 \tag{3}$$

The first two reactions take place at a pressure of 100 bar and at a temperature 423-453 K and it requires a energy of 37-47 kJ/mol-H_2 [2, 3, 4]. The third reaction however occurs at temperatures of the order of 673 K and cannot be carried out with HT-PEMFCs which operate in the temperature range of 150-200°C.

In the present paper, we investigate the possibility of using the heat released by the HT-PEMFC for the desorption of sodium alanate in order to extract the hydrogen required to run the cell. The thermal energy extraction from the HT-PEMFC stack can be done using a separate coolant like thermic oil which gets heated as it passes through the fuel cell and exchanges its heat with as it passes through a heat exchanger/ special jacket arrangement of the metal hydride. This requires a separate coolant circuit. In view of this, in the present study, we consider the possibility of using cathode air itself to serve the triple purpose of delivering oxygen to the fuel cell, cooling the stack and supplying the heat required for the desoprtion of the metal hydride. This has been done using a computational fluid dynamics (CFD)-based simulation of the flow and heat transfer within the various constituents of the stack. The details of the CFD model and the results obtained are discussed below.

2. Model description

The HT-PEMFC stack is assumed to consist of cells connected in series with one cooling plate for every four cells. For simplicity, the cooling plate is assumed to be having parallel channels which are of the same dimension as the parallel channel configuration on the flow field plates. Air enters the cooling plate at a temperature of 30°C at a stoichiometric factor to be determined. It gets heated as it flows through the cooling plate, thus extracting heat from the hot cells surrounding the cooling plate. At the exit of the cooling plate, the hot air would go through the desorption section of the metal hydrate unit and would give up heat to the metal hydride. The cooler exit gas from the metal hydride would then be fed through the cathode side of the fuel cells where they supply oxygen and in the process get also heated, again extracting heat from the cells. The objective is to see that in this process sufficient heat is given to the desorption unit to generate the required amount of hydrogen while keeping the cells (including the

catalyst layers and the membranes) sufficiently warm so that the electrochemical performance does not degrade but not so hot that the materials themselves degrade.
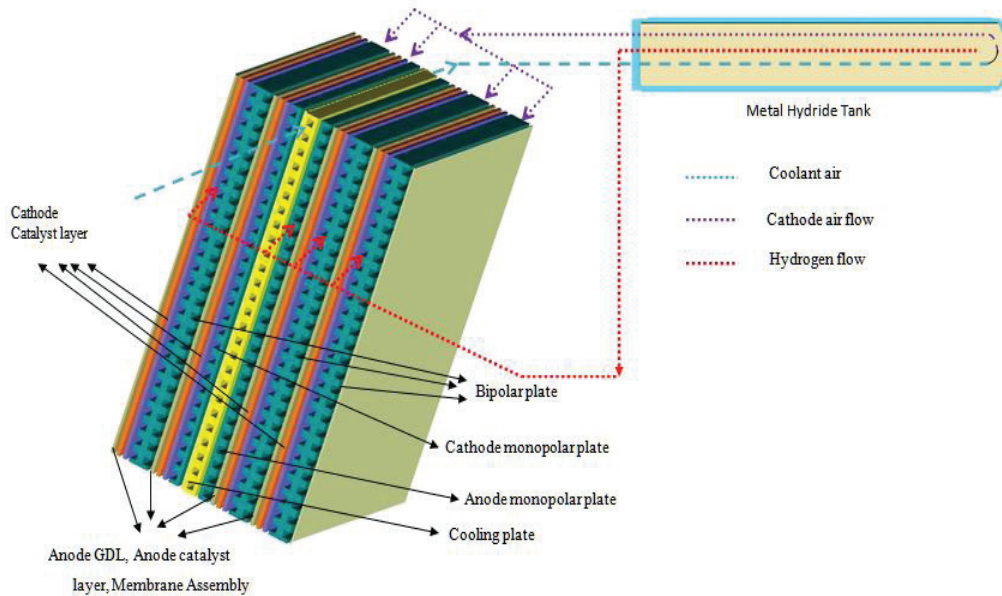

Fig. 1. Schematic diagram of a portion of the fuel cell stack showing the arrangement of one cooling plate for every four cells with combination of metal hydride tank.

This situation is modeled in the present study as follows. In a stack with one cooling plate for every four cells, two cells are located to the left of the cooling plate and other two cells are located at the right of the cooling plate as the shown Figure 1.

Further, each cell consists of different layers like the anode gas diffusion layer (AGDL), the cathode gas diffusion layer (CGDL), the anode catalyst layer (ACL), the cathode catalyst layer (CCL), the bipolar plate and the electrolytic membrane. Since the present problem is primarily concerned with conductive heat transfer within the sandwich of these layers, the AGDL, the ACL and the membrane, all of which have roughly the same thermal conductivity, are modeled as a single layer with an equivalent thickness. The anode flow channel is distinguished separately as a solid material of a different thermal conductivity. Since heat is generated at the catalyst sites at which the electrochemical reaction is taking place, and since the cathode overpotential is much larger than that on the anode, the cathode catalyst layer is treated as a volumetric heat source for the cell.

For the simplicity we have taken the computational domain to consist of half of the portion of the cooling plate and the adjacent two cells. This has the following dimensions: thickness in the x-direction of 9.557mm, height in the y-direction of 2 mm and length in the flow (z-) direction of 100 mm. The y-direction is a repeating unit of parallel flow channel in the stack and the z-direction is the flow direction of the coolant in the cooling plate and opposite to cathode air flow. The hydrogen desorption unit is

modeled as a heat sink term applied on the channel connecting the cooling plate and the individual cathode flow channels on the cells. This connecting channel is thus located outside of the stack area. The flow domain consists of one air flow inlet (into the coolant plate) and two air flow outlets, one each in the cathode flow fields. All the other surfaces are modeled either as walls or as symmetry planes, as appropriate. Convective heat transfer boundary condition has been applied on the surfaces exposed to outside atmosphere. The dimensions and properties etc used correspond to those used in our earlier work [7].

Due to convection and conduction, there will be temperature variation within the cell. This will have an effect on the polarization curve and the current density therefore will not be uniform. This effect has been modelled as follows. The variation with temperature of the local current density and the strength of the local volumetric heat source are formulated as follows. The cell voltage can be expressed in terms of various polarization losses by using following empirical formula [5, 6]:

$$V_{cell} = \frac{V_0 - RT_{cell}}{4\alpha_c F} \ln\left(\frac{i_{cell} + i_0}{i_0}\right) - \frac{R_{ohmic} i_{cell} - R_{con} i_{cell}}{\lambda - 1} \tag{4}$$

where α_c is the cathode transfer coefficient, i_o is the exchange current density, R_{ohmic} and R_{conc} are the ohmic and concentration losses (expressed as equivalent resistances) and λ is the stoichiometric factor.

The varying current density, volumetric heat source values with temperature are calculated as follows [7]. The current density variation as the function of temperature a constant voltage of 0.6 V can be expressed as:

$$i_{cell} = 1.377 \times 10^{-7} T_{cell}^3 - 0.0001767 T_{cell}^2 + 0.07855 T_{cell} - 11.77 \tag{5}$$

The amount of heat produced from the single cell is formulated as follows. The enthalpy of water formation in gaseous phase, $\Delta H_{g,T}$, can be evaluated as

$$\Delta H_{g,T} = \Delta H_l^f - \Delta H_T^{vap} \tag{6}$$

where the enthalpy of water formation in liquid phase, ΔH_l^f, is 285830 J and the heat of vaporization of water, ΔH_T^{vap}, is evaluated from [8] the following equation

$$\Delta H_T^{vap} = 3.6985 x 10^{-4} T_{cell}^3 - 0.4834 T_{cell}^2 - 152.4258 T_{cell} + 68260.5789 \tag{7}$$

where ΔH_T^{vap} is in Joule and T_{cell} in K.

From equations (1-8), the total heat released from each cell in the stack can be written as

$$Q_{cell} = \left(-\frac{\Delta H_{g,T}}{nF} - V_{cell}\right) i_{cell} \tag{8}$$

and the total amount of heat released from the stack can be written as

$$Q_{st} = Q_{cell} N_{cell} \tag{9}$$

3. Results and discussion

The simulation was carried at a cell voltage of 0.6 V with taking account constant current density and varying current density. The operating and design parameters for the 1-kWe HTPEMFC stack are shown in Table 1. The calculations leading to the evaluation of the minimum and the maximum amount of energy needed for the metal hydride tank to release one stoichiometric ratio of hydrogen are shown in Table 2. The heat sink term was applied with a maximum of energy 0.41 W and a minimum energy of 0.32 W required to release the hydrogen form a sodium alanate.

Table 1. Properties and design parameter of a 1-Kwe HT-PEMFC stack.

Desired power output (p_{st})	1000	watts
Cell active area (A_{cell})	0.01	m^2
Cell voltage (v_{cell})	0.60	v
Cell current density (i_{cell})	4200	A/m^2
Cell operating temperature (T_{st})	473	K
Maximum temperature form Cooling plate out (T_{cpch})	461	K
Inlet temperature coolant (T_{in})	300	K
Stack current (I)	42	A
Stack Voltage (V_{st})	24	V
Number of cell (N_{cell})	40	
Heat of produced from stack	913	W
Minimum amount of energy required for hydrogen desorption from NaAlH$_4$	36700	J/mol
Maximum amount of energy required for hydrogen desorption from NaAlH$_4$	46600	J/mol

Table 2. Mass and energy balance of 1kWe HT-PEMFC stack with metal hydride tank

	Stoichiometric factor H2 is equal 1		
	Simulated Slice	Single cell	Stack
H2 required (mol/sec)	8.71×10^{-06}	2.18×10^{-04}	9.14×10^{-03}
Minimum heat required (W)	0.32	7.99	336
Maximum heat required (W)	0.41	10.14	426
Approximately amount of heat produced (W)	0.91	22.93	913

3.1. Constant current density

In this case we have taken the cell voltage as 0.6 V and the (constant) current density as 0.42 A/cm^2. Figure 2 shows that for a given heat sink, the maximum temperature occurs in the catalyst layer and it decreases as the stoichiometric ratio of air increases. A stoichiometric ratio of air 5.5 is needed in order to

cool the stack at a heat sink value of 0.32 W and a stoichiometric ratio of air 4.75 is needed for a heat sink value of energy 0.41 W.
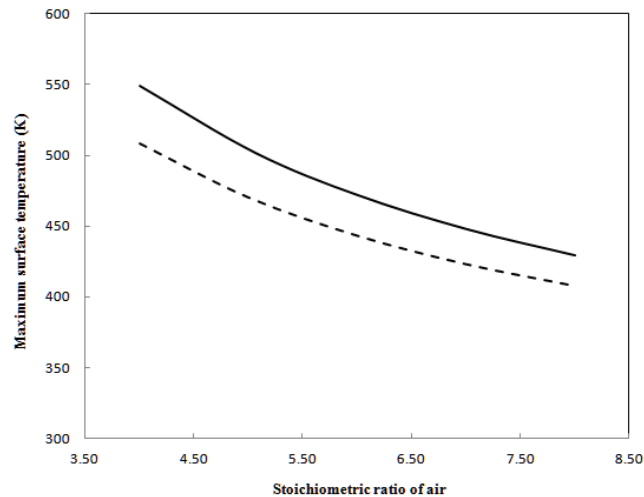

Fig. 2. Variation of the maximum surface temperature with the stoichiometric factor for energy required to release hydrogen from metal hydride minimum energy (solid line) and maximum energy (dashed line) at current density of 0.42 A/cm^2.

When there is no heat sink (that is when no heat is used for hydrogen desorption), a stoichiometric factor of 10 needed [7] and the temperature variation over the catalyst layer is also higher. The coolant coming out from the cooling plate is partially cooled in the hydrogen desorber (modeled here as a heat sink term) and it is again sent though the cathode air flow channels. As the cathode air flows through the channel, it absorbs heat from the solid surface and thus reduces the difference between maximum to minimum surface temperature (ΔT_{cat1}, ΔT_{cat2}) of the catalyst layers. The ΔT_{cat1}, ΔT_{cat2} decreases as the stoichiometric factor of air increases as shown in Tables 3 and 4. As expected, ΔT_{cat1}, ΔT_{cat2} values are higher when the heat sink value is higher and the inlet temperature of the cathode air channel is lower.

Table 3. Temperature Variations in the stack when minimum amount of energy condition applied as a heat sink.

Stoichiometric ratio of air	Velocity (m/sec)	Inlet temperature of the cathode air (K)		Outlet temperature of the air (K)			Maximum to minimum surface temperature of the catalyst layers (K)		Average temperature of the catalyst (K)
		T_{Bch1}	T_{Bch2}	T_{CP}	T_{Bch1}	T_{Bch2}	ΔT_{cat1}	ΔT_{cat2}	
10.19*	10.00	458	458	461	446	449	45	36	463
4.00	3.93	436	412	536	524	527	38	30	538
5.00	4.97	405	393	489	480	483	33	25	492
6.00	5.89	384	379	459	453	456	28	21	464
7.00	6.87	368	367	435	432	434	24	21	441
8.00	7.85	355	357	416	415	417	21	21	423

* Without thermal coupling with metal hydride (heat sink value is zero).

Table 4. Temperature Variations in the stack when maximum amount of energy condition applied as a heat sink.

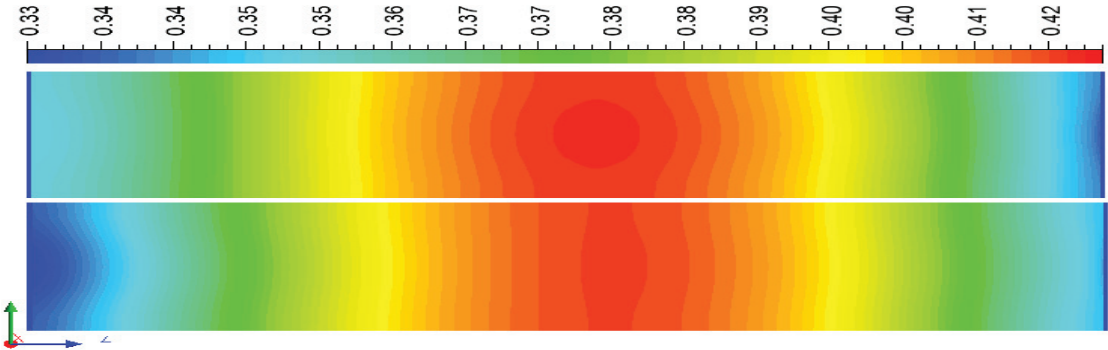| Stoichiometric ratio of air	Velocity (m/sec)	Inlet temperature of the cathode air (K)		Outlet temperature of the air (K)			Maximum to minimum surface temperature of the catalyst layers (K)		Average temperature of the catalyst
		T_{Bch1}	T_{Bch2}	T_{CP}	T_{Bch1}	T_{Bch2}	ΔT_{cat1}	ΔT_{cat2}	(K)
4.00	3.93	361	331	488	488	490	30	35	499
5.00	4.91	343	328	451	452	455	28	33	462
6.00	5.89	330	323	425	428	430	27	31	435
7.00	6.87	320	319	405	410	412	26	30	416
8.00	7.85	312	315	389	396	397	26	29	401

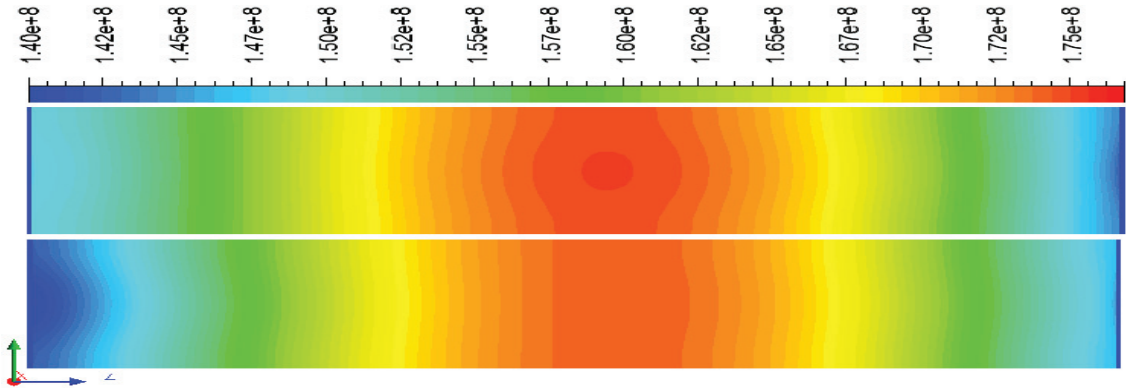Fig. 3. The spatial variation of the current density in the catalyst layers

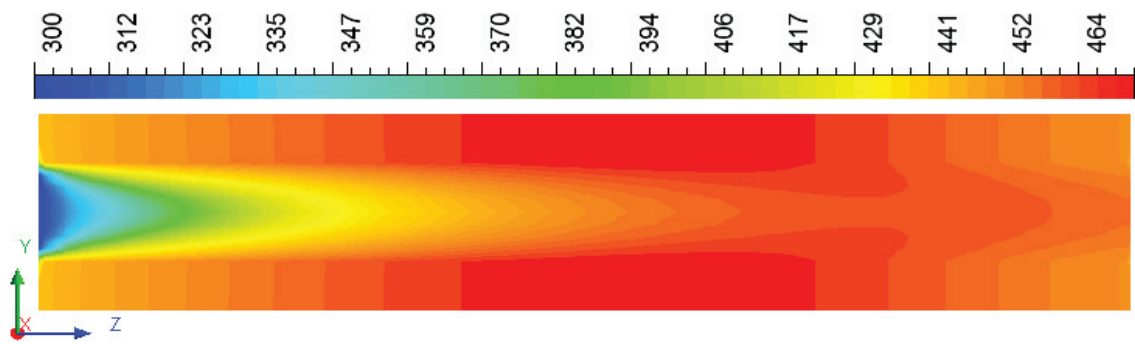Fig. 4. The spatial variation of heat source in the catalyst layers

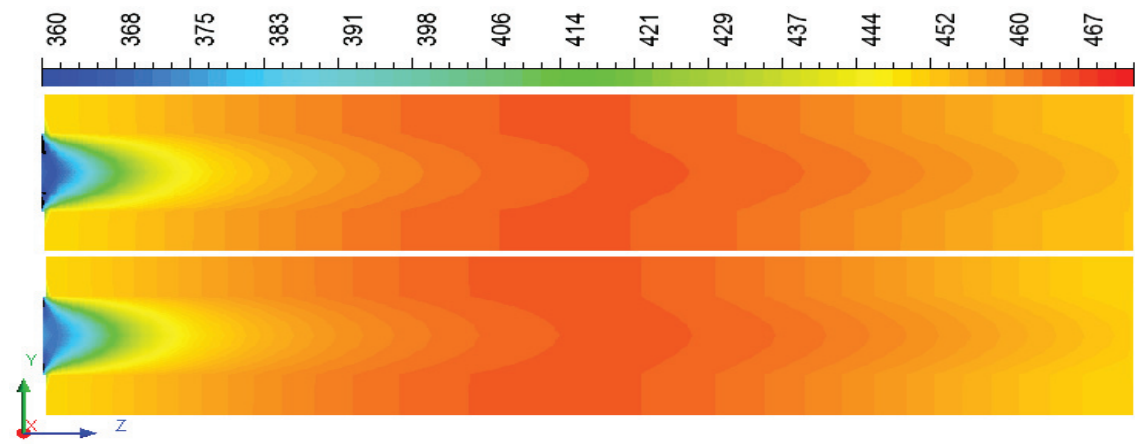Fig. 5. (a) The spatial variation of the temperature in the cooling plate channel.

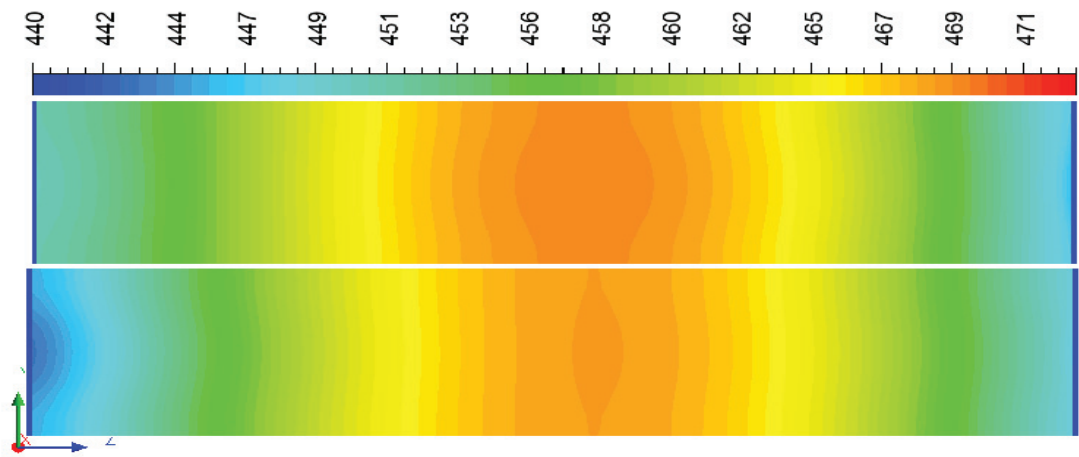Fig. 5. (b)   The spatial variation of the temperature in the bipolar plate channels.

Fig. 5. (c) The spatial variation of the temperature in the catalyst layers.

3.2. *Varying current density*

The current density highly influenced by temperature and it is varying along the length of the channel. The varying current density, volumetric heat source values with temperature are calculated by using equations [4-9]. The maximum current density 0.42 A/cm^2 is obtained at cell temperature of 473 K and it decreases as a function of the cell temperature. The spatial variations in the heat source and local current density of the catalyst layers are shown in Figures 4 and 5 and the corresponding variations in the temperature of the catalyst layer, bipolar plate channel and cooling plate channel are shown in Figure 6 at a stoichiometric factor of 4.84 (with a heat sink value of 0.32 W). It may be noted that Figures 4, 5 and 6 have been scaled in the z-direction by a factor of 10 in order to improve clarity. The catalyst layer-1 which is near to the cooling plate has lower surface temperature as compared to the catalyst layer-2 which is farther. The solid temperature in the middle portion of the stack is high compared to the edges of the stack because the cooling plate air, bipolar plate air are flowing in opposite direction to each other within the stack. At a stoichiometric factor of 4.84 ΔT_{cat1} =25 K, ΔT_{cat2}=26 and corresponding current density, heat source and the temperature variations are shown in Figure 7. At the entrance of the bipolar plate channel, the inlet temperature are very low due to the thermal energy taken away for the desorption of hydrogen. As the air flows through the bipolar plate from the inlet to the outlet of the channel, it gains temperature continuously up to a length of z=0.07 m (which is at a distance of 0.03 m form the edge of cooling plate entrance) and after that the temperature in the bipolar plate channel decreases. The temperatures in the solid layers are varying by about 28 K along the flow path.
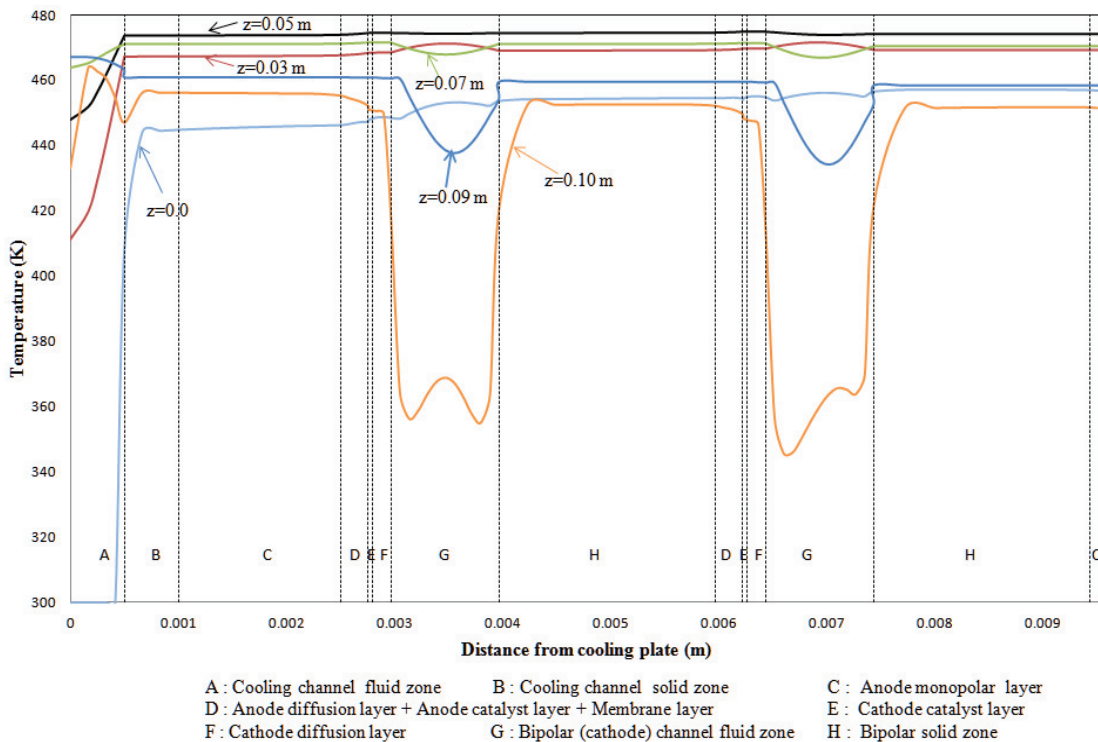

Fig. 6. Temperature variations along the stack thickness (one cooling plate with two cells) at a stoichiometric factor of 4.84 after the energy utilized for H$_2$ desorption form metal hydride.

The predicted temperature within the catalyst layers is in the range of 440-471 K forming a relatively hot spot in the middle of the catalyst and while the edges of the catalyst layer have a cold region. The current density on the catalyst layer is varying from the 0.33 A/cm^2 to 0.42 A/cm^2 with an average of 0.39 A/cm^2. The local current density value is varying by about $\pm$ 15% from the average current density value. Thus, the extractable power decreases by about 7% from the case of uniform current density due to temperature variation over the cell.

4. Conclusions

The amount heat produced from the 1 kWe stack at a voltage 0.6 V is approximately three times higher than the amount heat required for NaAlH$_4$ to desorb hydrogen from the metal hydride. The calculations shows that, with a cathode air flow rate seven times in excess of the stoichiometric requirement, it is possible to meet the triple requirement of supplying preheated cathode air if stack is assumed running at constant current and constant voltage. When local current density variation across the catalyst layer is considered, the stoichiometric factor of air gets reduced to 4.84. The combination of thermal management HT-PEMFC, metal hydride with using air thus appears viable.

References

[1] Zhang J, Tang Y, Song C, Zhang J, Polybenzimidazole membrane based PEM fuel cell in the temperature range of 120–200°C. *J Power Sources* 2007; **72** : 163-171.

[2] Ahluwalia R, Hua T, Peng J. On-board and Off-board performance of hydrogen storage options for light-duty vehicles. *Int. J. Hydrogen Energy* 2011; **37**:2891–10.

[3] Pfeifer P, Wall C, Jensen O, Hahn H, Fichtner M. Thermal coupling of a high temperature PEM fuel cell with a complex hydride tank. *Int. J. Hydrogen Energy* 2009; **34**:3457-66.

[4] Førde T, Eriksen J, Pettersen A, Vie P, Ulleberg Ø. Thermal integration of a metal hydride storage unit and a PEM fuel cell stack. *Int. J. Hydrogen Energy* 2009; **34**: 6730-39.

[5] Korsgaard AR, Refshauge R, Nielsen MP, Bang M, Kær SK. Experimental characterization and modeling of commercial polybenzimidazole-based MEA performance,. *J. Power Sources* 2006;**162 :** 239 – 245.

[6] Korsgaard AR, Nielsen MP, Bang M, Kær SK., Modeling of co influence in PBI electrolyte PEM fuel cells, *The 4th International Conference on Fuel Cell Science, Engineering and Technology* 2006; June 19-21, 2006, Irvine, CA.

[7] Reddy EH, Jayanti, S. Thermal management strategies for a 1 kWe stack of a high temperature proton exchange membrane fuel cell. *Appl. Therm. Eng* 2012; **48**:465-475

[8] Scott K, Mamlouk M. A cell voltage equation for an intermediate temperature proton exchange membrane fuel cell, *Int J Hydrogen Energy* 2009; **34**: 9195–9202.